ARMY RESEARCH LABORATORY

Optimization of $PbTiO_3$ Seed Layers for PZT MEMS Actuators

by Luz Sanchez and Ronald G. Polcawich

ARL-TR-4697 **December 2008**

NOTICES

Disclaimers

The findings in this report are not to be construed as an official Department of the Army position unless so designated by other authorized documents.

Citation of manufacturer's or trade names does not constitute an official endorsement or approval of the use thereof.

Destroy this report when it is no longer needed. Do not return it to the originator.

Army Research Laboratory
Adelphi, MD 20783-1197

ARL-TR-4697 **December 2008**

Optimization of $PbTiO_3$ Seed Layers for PZT MEMS Actuators

Luz Sanchez and Ronald G. Polcawich
Sensors and Electron Devices Directorate, ARL

REPORT DOCUMENTATION PAGE	Form Approved OMB No. 0704-0188

1. REPORT DATE *(DD-MM-YYYY)*	2. REPORT TYPE	3. DATES COVERED (From - To)
December 2008	Summary	May to September 2008

4. TITLE AND SUBTITLE

Optimization of $PbTiO_3$ Seed Layers for PZT MEMS Actuators

5a. CONTRACT NUMBER

5b. GRANT NUMBER

5c. PROGRAM ELEMENT NUMBER

6. AUTHOR(S)

Luz Sanchez and Ronald G. Polcawich

5d. PROJECT NUMBER

5e. TASK NUMBER

5f. WORK UNIT NUMBER

7. PERFORMING ORGANIZATION NAME(S) AND ADDRESS(ES)

U.S. Army Research Laboratory
ATTN: AMSRD-ARL-SE-RL
2800 Powder Mill Road
Adelphi, MD 20783-1197

8. PERFORMING ORGANIZATION REPORT NUMBER

ARL-TR-4697

9. SPONSORING/MONITORING AGENCY NAME(S) AND ADDRESS(ES)

10. SPONSOR/MONITOR'S ACRONYM(S)

11. SPONSOR/MONITOR'S REPORT NUMBER(S)

12. DISTRIBUTION/AVAILABILITY STATEMENT

Approved for public release; distribution unlimited.

13. SUPPLEMENTARY NOTES

14. ABSTRACT

The material properties of sol-gel lead zirconate titanate (PZT) are inherently linked with its crystallinity and texture. The use of seed layers and control of the base metal crystal structure ultimately controls the ferroelectric and piezoelectric properties of the thin film. This effort attempted to transfer the $PbTiO_3$ seed layer fabrication process that has been recently accomplished at Pennsylvania State University under a fiscal year 2007 (FY07) Army Research Office – Short Term Innovative Research (ARO-STIR) project to the U.S. Army Research Laboratory (ARL). Characterization included x-ray diffraction and ferroelectric, dielectric, and piezoelectric properties of the PZT thin films and PZT actuators fabricated using the ARL piezo-microelectromechanical systems (MEMS) switch fabrication process.

15. SUBJECT TERMS

PZT, thin film, $PbTiO_3$, seed layer

16. SECURITY CLASSIFICATION OF:			17. LIMITATION OF ABSTRACT	18. NUMBER OF PAGES	19a. NAME OF RESPONSIBLE PERSON
a. REPORT	b. ABSTRACT	c. THIS PAGE	UU	30	Ronald G. Polcawich
U	U	U			19b. TELEPHONE NUMBER (*Include area code*) (301) 394-1275

Standard Form 298 (Rev. 8/98)
Prescribed by ANSI Std. Z39.18

Contents

List of Figures

List of Tables

Acknowledgment

We would like to acknowledge the work of Richard Piekarz and Joel Martin of the U.S. Army Research Laboratory (ARL) and Brian Power of General Technical Services for their contributions in the training and fabrication of the lead zirconate titanate (PZT) capacitor and cantilever structures.

INTENTIONALLY LEFT BLANK.

1. Introduction/Background

Microelectromechanical systems (MEMS) will become one of the leading technological devices of the future. Although they are already on the market as pressure and inertial sensors (*1*) (i.e., accelerometers in modern cars for airbag deployment), the goal is to use them in almost all everyday applications from data storage in computers to drug delivery devices. Depending on the device and applications of interest, there are a variety of different materials and manufacturing techniques available.

With a wide range of applications for MEMS devices, one of the applications of interest is millimeter-scale robotics. The size of these devices makes it unreasonable to use motor like systems, the surface forces are stronger than the inertial forces. To overcome this obstacle, there is a need to create large force, large displacement actuators. Actuators based on piezoelectric materials are ideally suited to this application space. Piezoelectricity was discovered in the 1880s by Jacques and Pierre Currie on a piece of quartz. In a piezoelectric material, there is a relationship between a material's electrical and mechanical behaviors (i.e., if we apply a voltage across the surface of a piezoelectric material, there will be a physical change in that material, either by bending or changing its length).

The material used in this study, lead zirconate titanate (PZT), exhibits piezoelectric properties. PZT is one of the most economical piezoelectric ceramics, making it cost effective for mass production. It also exhibits a high piezoelectric coefficient (*2*) allowing for the use of lower voltages to achieve the same actuator performance metrics. Figure 1 shows a unit cell of PZT, above and below the Curie temperature (>365 °C). At temperatures below the Curie point, the titanium (Ti) or zirconium (Zr) atom shifts away from the center of the unit cell creating a dipole (*3*). In an actual layer of PZT, there are hundreds of these dipoles pointing in different directions. By poling the samples with an electric charge, they can be reoriented to one general direction. After poling, the samples will retain the net dipole orientation unless degraded by exceeding the limits of the material.

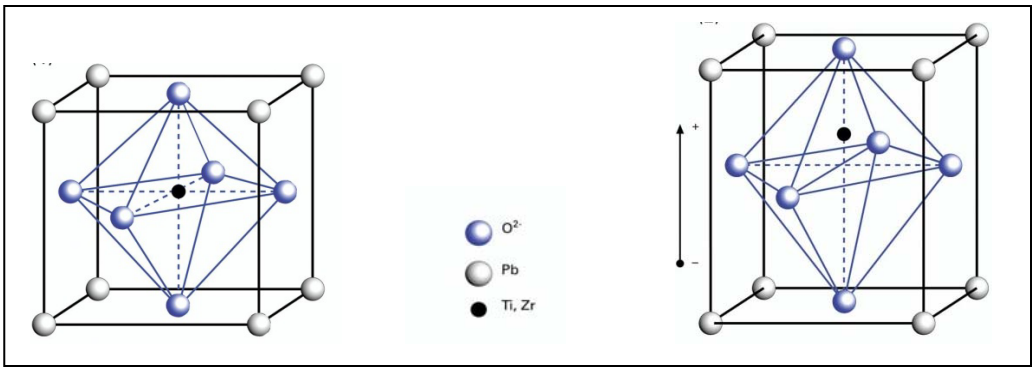

Figure 1. Piezoelectric effect at the molecular level: above the Curie temperature it is in a symmetric cubic state (left), and below the Curie temperature it is tetragonally distorted with a dipole moment (right) (*3*).

The piezoelectric coefficient of PZT thin films is inherently linked to its crystalline quality (*4*). After several different studies to increase the piezoelectric coefficient of sol-gel deposited PZT thin films, researchers at Pennsylvania State University (PSU) have developed a new method using a sol-gel derived $PbTiO_3$ seed layer based on the work of Muralt et al. (*5*). This seed layer has "good lattice matching with PZT film and a strong propensity for development of (001) orientation" (*6*). PZT oriented in the (001) direction has shown a near doubling of the piezoelectric coefficient. Using the $PbTiO_3$ seed layer and taking into account other parameters during production should produce well-oriented PZT films (*7*). In this work, the results from PSU will be adapted to the current sol-gel PZT process to analyze the effectiveness of using a seed layer as a template for creating (100) oriented PZT thin film actuators with superior piezoelectric coefficients.

2. Experiment/Calculations

2.1 PZT Preparation

Inside a controlled atmosphere glove box, we prepared a solution of lead acetate and 2-Methoxyethanol (2-MOE) using 37.3 g of lead acetate trihydrate powder poured into a 1 L flask and 120 mL of 2-MOE. The 2-MOE was poured into the flask with the weighing boat used to measure the lead acetate trihydrate, ensuring all residual lead acetate trihydrate was in the flask. The flask was clamped shut for vacuum distillation outside of the glove box.

A solution of Zr, Ti, and 2-MOE was prepared prior to the lead acetate vacuum distillation. For this solution, 20.5 mL of Zr n-propoxoide was poured into a 125 mL flask followed by 12.9 mL of Ti iso-propoxide and 45 mL of 2-MOE. A magnetic stirrer was dropped into the flask and then sealed and placed onto a stir plate while we proceeded with the vacuum distillation of the lead acetate solution.

A Heidolph Laborata 4000 rotary evaporator was used for the vacuum distillation. The flask was attached to the rotary evaporator and the system was pressured with a positive pressure of nitrogen (N_2) gas (allowed to flow out of a relief valve). The flask, now attached to the unit, was lowered to a 120 °C preheated silicone oil bath and allowed to rotate at 120 rpm. The N_2 gas was turned off and a vacuum was applied to the system allowing it to rotate for 20 min in a 410 mbar vacuum. As the solution is rotating in the oil bath, water vapor and 2-MOE is evaporated and rises into the cooling coils in the unit. It is then condensed and drops into a collection flask located under the cooling coils. After approximately 20 min, the lead acetate solution will suddenly change into white foam. At this point, the rotation was reduced to 35 rpm, the apparatus was raised out of the silicon oil bath, and the vacuum was removed by applying N_2 gas into the system. Once the system reached atmospheric pressure, the flask was removed from the rotary evaporator and submerged in water until it reached room temperature.

The lead acetate solution was taken back into the glove box where the Zr/Ti solution was added to it. An additional 70 mL of 2-MOE was poured into the Zr/Ti flask to gather any remaining solution and then poured into the lead acetate flask. This step was repeated one more time; for a total of 140 mL of 2-MOE. The flask, with the lead acetate and Zr/Ti solution, was sealed and removed from the glove box for vacuum distillation.

Once the 1 L flask was attached to the distillation unit, the unit was lowered into the silicon oil bath and rotated at 120 rpm. The unit was allowed to rotate for 3.5 h at 120 °C. After the 3.5 h, a 5 min vacuum was applied followed by the introduction of N_2 gas for 5 min. The flask was removed from the hot oil bath and cooled by submerging the sealed flask in water until it reached room temperature. The amount of solution in the flask was measured and compared against the target value of 250 mL. The solution was transferred into a storage container with the stirring magnet and 8.8 mL of formamide (4 volume %) was slowly added into the solution to act as a drying control agent. The PZT container was sealed and placed on the stirring plate overnight (*9*).

2.2 $PbTiO_3$ Seed Layer Solution

Preparing the $PbTiO_3$ solution required the same process used to make PZT. We used 16.27 g of lead acetate trihydrate and mixed it with 120 mL of 2-MOE, once again ensuring all of the lead acetate trihydrate powder was placed into the 1 L flask. In a separate flask, 9.96 mL of Ti iso-propoxide with 45 mL of 2-MOE was mixed and allowed to stir while vacuum distillation was performed on the lead acetate solution, similar to the process used to PZT (without the additive

of the Zr precursor). Once the vacuum distillation of the lead acetate solution was done, the Ti iso-propoxide solution was added to the lead acetate solution inside of the glove box. After this step, all the same steps mentioned in section 2.1 were followed.

Based on discussions with the research group at PSU, the procedure to test the $PbTiO_3$ seed layer (PT seed layer) required two different solutions, one with acetic acid and one without. Improved results with acetic acid were reported by PSU researchers (*8*). For samples without the addition of acetic acid, the PT seed layer was used once it finished stirring overnight. For the samples that did require acetic acid in the PT seed layer solution, 14 mL of the PT seed solution was poured into a storage container with a magnetic stirrer and 1 mL of acetic acid was added to this solution and allowed to mix for 10 min.

2.3 Preparation Prior to Sol-Gel Processing

Using blank single-sided polished 100 mm silicon wafers, a 2000 Å thick silicon dioxide layer was deposited using a Plasma Therm 790 plasma enhanced chemical vapor deposition (PECVD) system. To ensure a thickness of 2000 Å, a J.A. Woollam spectroscopic ellipsometer was used to measure the thickness across the wafer. Once the thickness was confirmed, the wafers were annealed using an A.G. Associates Heat Pulse 610 Rapid Thermal Anneal (RTA) furnace at 700 °C for 60 s in flowing N_2 gas. Next, a sputter deposited bi-layer of Ti/platinum (Pt) was deposited using a Unaxis Clusterline 200 system. The bilayer consisted of 200 Å of Ti and 850 Å of Pt. After depositing the Ti/Pt bottom electrode, the wafers were ready for the PZT sol-gel processing.

2.4 Sol-Gel Processing

Initial testing was performed on eight 1-in. square samples followed by testing on four 100 mm wafers, as will be discussed in the next couple of sections. A series of 1-in. test samples was used to determine an effective method to reproduce the data from the previous work by PSU. Two control samples with varying Zr/Ti ratios were used, PZT (45/55) and PZT (52/48), and compared with six test samples with the varying PT seed layer conditions and using either PZT (45/55) or PZT (52/48). Table 1 lists each of the samples along with a description of the pertinent processing information.

Table 1. $PbTiO_3$ test sample summary.

Initial $PbTiO_3$ Seed Layer Tests			
1. Control Sample 1	• 45/55 PZT 5000Å • No PT Seed Layer • 700 °C RTA	**2. Control Sample 2**	• 52/48 PZT 5000Å • No PT Seed Layer • 700 °C RTA
3. Seed Test 1-Sample 1 with Acetic Acid	• PT Seed 200 Å • 700 °C RTA • 45/55 PZT 5000Å • 700 °C RTA	**4. Seed Test 1-Sample 2 with Acetic Acid**	• PT Seed 200 Å • 700 °C RTA • 52/48 PZT 5000Å • 700 °C RTA
5. Seed Test 2-Sample 1 with Acetic Acid	• PT Seed 200 Å • 600 °C RTA • 45/55 PZT 5000Å • 700 °C RTA	**6. Seed Test 2-Sample 2 with Acetic Acid**	• PT Seed 200 Å • 600 °C RTA • 52/48 PZT 5000Å • 700 °C RTA
7. Seed Test 3-Sample 1 without Acetic Acid	• PT Seed 200 Å • 600 °C RTA • 45/55 PZT 5000Å • 700 °C RTA	**8. Seed Test 3-Sample 2 without Acetic Acid**	• PT Seed 200 Å • 600 °C RTA • 52/48 PZT 5000Å • 700 °C RTA

The two control samples used the existing process for depositing sol-gel PZT thin films and will be described in this section. Using a 10 mL syringe filled with the PZT solution along with a 0.1 µm filter, the solution was statically dispensed onto the surface of the test specimen. The sample was spun for 45 s at 2500 rpm and then pyrolyzed on a hot plate with vacuum for 2 min at 350 °C. Following pyrolization, the film was crystallized using the RTA (specifically used for PZT samples) for 60 s at 700 °C in a 4 °C/s ramp in flowing oxygen. The deposition steps were repeated 7 or 8 times until the PZT measured approximately 5000 Å using a J.A. Woollam spectroscopic ellipsometer.

The sol-gel process for the samples using a PT seed layer was a little different. Four of the test samples required a PT seed layer with acetic acid and two of them required no acetic acid. Prior to the PZT deposition, the samples were coated with a single layer of the PT seed layer solution with a targeted thickness of 200 Å. The seed layer was statically dispensed and then spun for 45 s at 2500 rpm and then pyrolyzed for 2 min at 350 °C. The samples were put into the RTA for 60 s to fully crystallize the film. The temperature of the RTA was either 700 °C or 600 °C depending on the sample (as shown in table 1). Following the seed layer crystallization, a 5000 Å PZT layer was deposited using the same process used for the control samples. The final film thicknesses for all eight test samples are outlined in table 2. Figure 2 diagrams the sol-gel process for control samples without a PT seed layer and test samples with a PT seed layer.

Table 2. Thickness values of the eight 1-in. test samples.

Sample	PT Seed Thickness	PZT Thickness (Å)
1	None	5001
2	None	5002
3	156	4968
4	214	5013
5	230	5098
6	228	5054
7	270	5272
8	280	5014

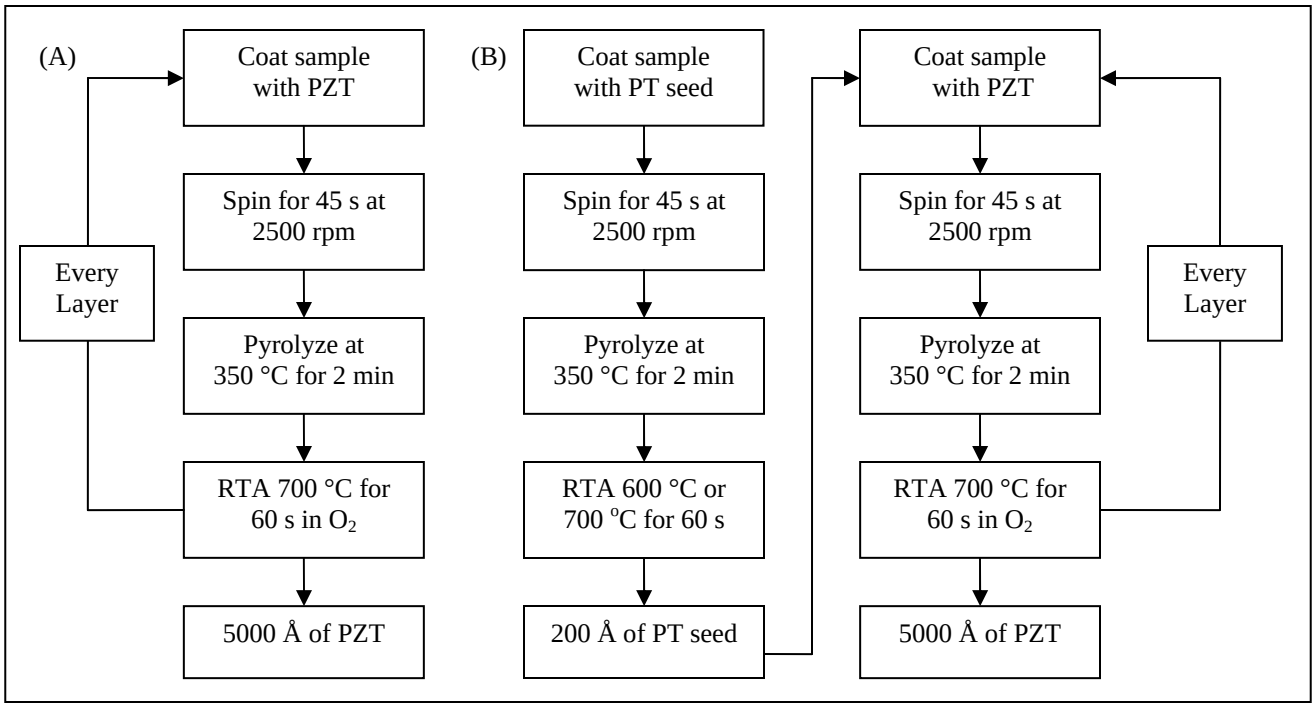

Figure 2. (a) The sol-gel process for control samples without a PT seed layer and (b) the sol-gel process for test samples with a PT seed layer.

2.5 Initial $PbTiO_3$ Seed Layer Tests

2.5.1 Photolithography

The initial tests with the seed layer involved coating PZT thin films on the 1-in. square test specimens. After the PZT deposition, the test samples underwent photolithography. The samples were coated with Clariant AZ5214E photoresist in a stationary spinner chuck and spun at 2000 rpm for 40 s. Spinning the sample allows for the application of a uniform layer of photoresist as the centrifugal forces expels excess resist from the edge of the sample (*10*). After the coating, the samples are placed on a hot plate for 60 s at 110 °C. The resist was exposed for 2.1 s under low vacuum contact using a Karl Suss MA/BA6 contact aligner using a test mask comprised of an array of 500 x 500 µm squares. After this first exposure, a post exposure bake

was performed at 120 °C for 30 s. Following the bake, a flood exposure of 3.5 s was done to achieve an image reversal to create a re-entrant sidewall profile. After exposure, the resist was developed using an AZ 300MIF developer for 75 s followed by inspection under a microscope.

2.5.2 Post Lithography

With the resist patterning complete, a top Pt layer was sputter deposited on the samples to serve as a top electrode during electrical testing of the PZT capacitors. The Pt was deposited using a Varian 3190 DC magnetron sputterer system to deposit approximately 1000 Å of Pt. After deposition, the samples were placed in an acetone bath to remove excess metal and resist using a liftoff technique. Using a resist with a re-entrant sidewall allows the Pt deposited in the 500 x 500 μm squares to be removed while the excess Pt and resist is removed. The liftoff process took approximately 30 min and then the samples were rinsed with methanol, isopropyl alcohol, and finally de-ionized water.

To open access to the bottom Pt, the samples were again coated with photoresist and the resist in one corner of the sample was removed with acetone. The open corner was then exposed to a wet etch solution to remove the PZT, thereby revealing the bottom Pt layer. The etch solution consisted of 240 mL of distilled water, 120 mL of hydrogen chloride (HCl), and 1 mL of hydrogen fluoride (HF). The area to be etched was dipped into the solution and agitated for several seconds until the bottom Pt electrode was visible and appeared clean. The sample was rinsed with liberal amounts of de-ionized water. After the wet etch process, the remaining resist was removed using oxygen plasma for 25 min.

2.6 $PbTiO_3$ Seed Layer Wafer Tests

After the initial electrical measurements on the eight 1-in. samples measured, the two best solutions were chosen to create four 100 mm wafers (two controls and two test samples). Processing on the 100 mm wafers allows for the fabrication of cantilever arrays used to evaluate the piezoelectric coefficient of the PZT thin film.

The fabrication of the cantilever arrays began with the deposition of an oxide-nitride-oxide (ONO) elastic layer on a 100 mm (100) silicon wafer. The bottom silicon dioxide was 2000 Å, the silicon nitride was 500 Å, and the top silicon dioxide was 2500 Å. Following deposition, the wafer was annealed at 700 °C for 60 s in flowing N_2. After the anneal, the thickness and residual stress were measured. Next, the bottom Ti/Pt bilayer (200 Å/820 Å) was sputter deposited at 500 °C using a Unaxis Clusterline 200. After the metal deposition, the PT and the PZT thin films were deposited following the procedure outlined in a previous section. Following the PZT deposition, a top 1050 Å Pt layer was sputter deposited at 300 °C using a Unaxis Clusterline 200. Figure 3 shows the composite stack prior to photolithography.

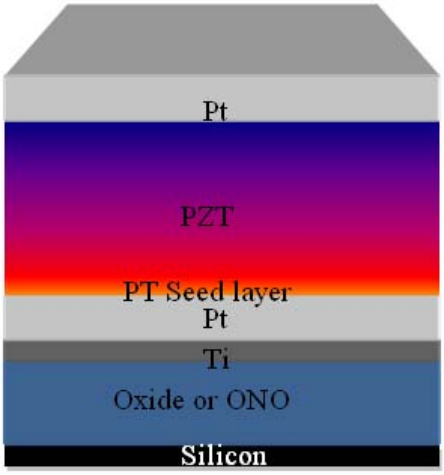

Figure 3. Composite stack prior to photolithography.

2.7 Photolithography

The Karl Suss ACS200 Wafer Coater/Developer was used to spin coat 4-in. test wafers with AZ5214E resist. Using the Karl Suss MA/BA6 Contact Aligner, a positive exposure on the top metal pattern was performed. The wafer was developed on the Karl Suss ACS200 using AZ300MIF developer. Resist was removed along the edge of the wafer, edge bead removal, in preparation for the ultraviolet (UV) cure. During the spinning process, surface tensions along the edge of the wafer cause a thicker layer of resist to be formed. This thickened layer will cause gases to be encapsulated during the UV cure process forming defects. A clean cloth moistened with acetone was placed in the hood and the wafer was rolled over the acetone to remove this resist. A 5-min descum using the Metroline/IPC Plasma Photoresist Stripper removed any unpatterned resist that remained on the wafer. The UV cure heats the wafer to soften the resist, which allows impurities to escape in gas form. The system then allows the resist to harden. This prepares the wafer for the first ion mill step in the procedure. During this process, the top Pt layer that is not covered with resist is removed, exposing the PZT beneath. After this process, the wafers underwent a 25 min ash that removed all the resist from the wafer. A PZT and bottom metal ion mill is performed after all the steps prior to the first ion mill are accomplished. By this point, alignment on the Karl Suss MA/BA6 Contact Aligner is crucial. Another 25 min ash was performed to remove all resist. Figure 4 shows the positive and reverse image photolithography.

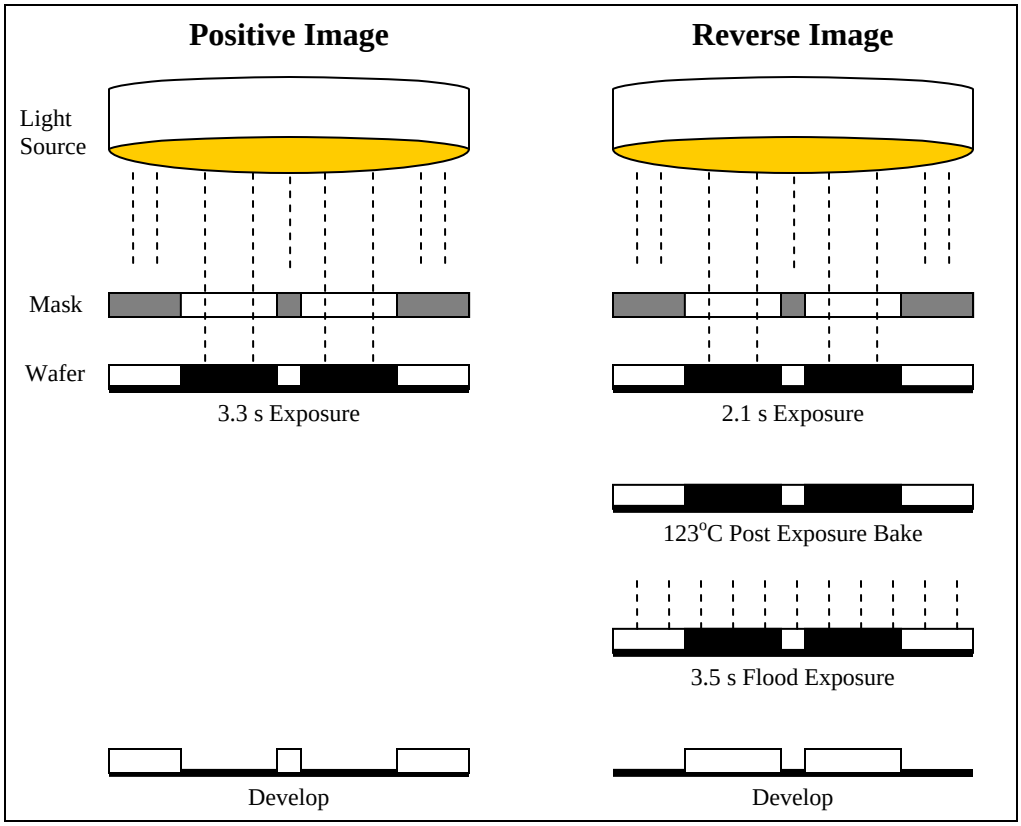

Figure 4. Positive and reverse image photolithography.

The ONO layer deposited earlier is now exposed after the second ion mill. However, the resist protected a portion of the PZT and bottom metal from ion milling in order to use the bottom metal as a contact point to apply a voltage across the cantilever array that is being formed. To expose the bottom metal, a PZT wet etch is performed after patterning the next part of the circuit with a reverse exposure of the AZ5214 photoresist. A new solution was made to ensure a quick and clean wet etch. The mixture was placed into a Teflon container into which a 4-in. wafer could fit and a similar glass container was filled with de-ionized water to end the reaction. The wafer was placed into the PZT wet etch mixture and agitated for 5–15 s. Color changes were observed on a large bottom metal pad; the wafer was immediately removed from the PZT wet etch mixture when this pad finished changing colors and was placed into the de-ionized water container. Water was allowed to run over the wafer to completely end the reaction and then it was dried using N_2 gas. The wafer was inspected to be sure that the PZT was completely etched through but that the circuit features were not damaged or over-etched since this could cause a short-circuit. A 25-min ash was performed to remove all resist from the wafer.

An oxide reactive ion etching (RIE) is performed on the exposed ONO. First, we patterned our next circuit features using resist, then a reverse exposure was performed, and a 5-min descum was done to remove unpatterned resist. The Lam 590 Oxide/Nitride Etch (Lam 590) bombarded

the sample with fluorine ions causing damage to the bonds and removing the ONO layers on the wafer. The sample was inspected to determine how far it was etched. After the etch, a 25-min ash was performed.

The final pattern was preparation for a Ti and gold (Au) deposition and used a reverse exposure. The Evatec BAK 641 Electron Beam Evaporator deposited 200 Å of Ti followed by 3000 Å of Au. This will protect the contact pads during electrical testing from getting scratched by the electrical probes. The entire wafer was covered with Ti and Au and an acetone liftoff was required to remove all Ti and Au that is attached to the resist. This results in Ti and Au staying only in the areas that were not covered with resist. A 5-min ash was performed to remove all resist from the wafer.

Throughout all the processes mentioned, the cantilever array was slowly being formed. The final step was to release the structures from the wafer. A final 20 s oxide etch was performed using the Lam 590 followed by a XeF_2 etch. This process etches the Si substrate and does not damage the other layers on the wafer.

Figure 5 shows all the processes step by step.

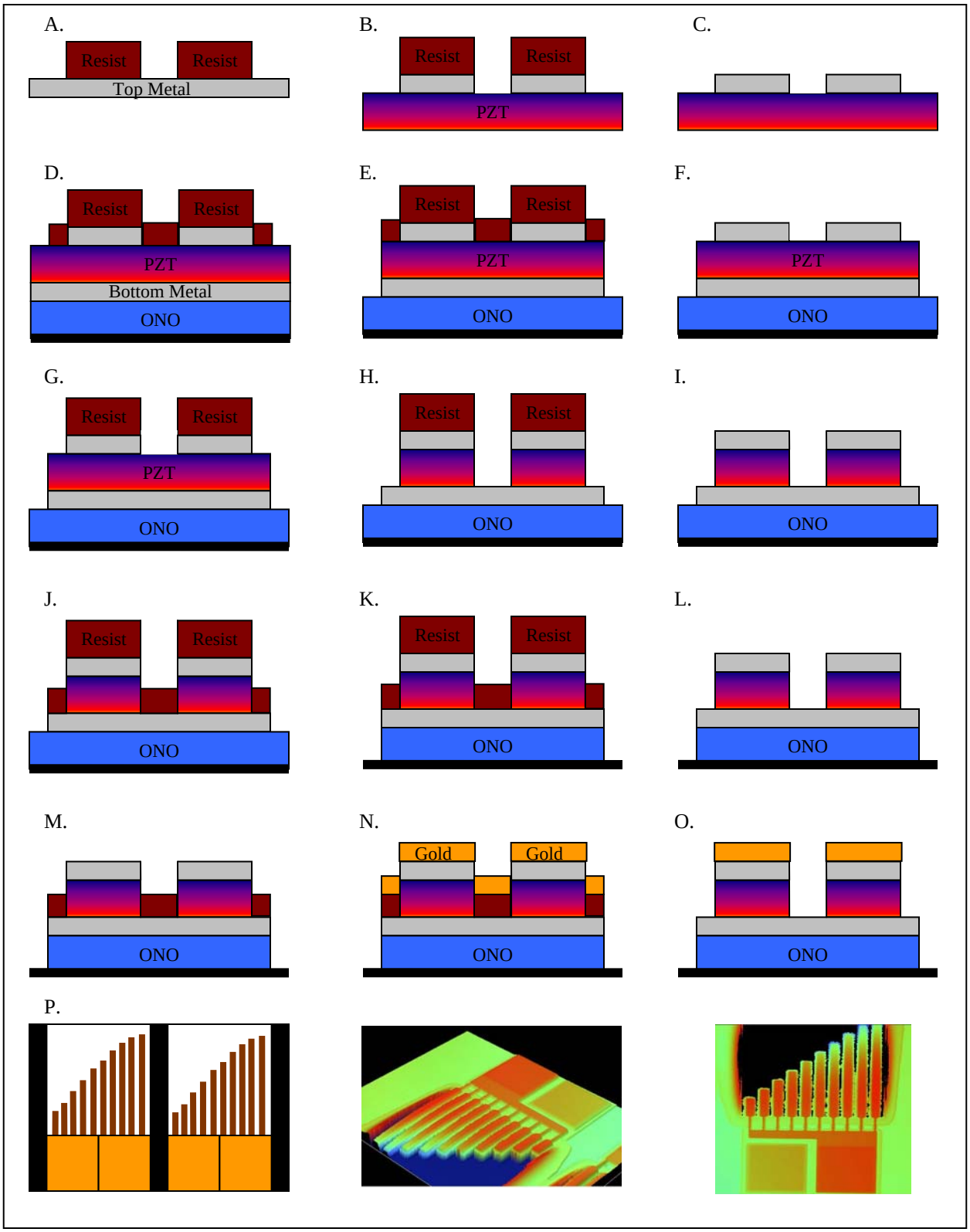

Figure 5. (a) Top metal pattern, (b) 1st ion mill, (c) After 25 min ash, (d) PZT/bottom metal pattern, (e) 2nd ion mill, (f) After 25 min ash, (g) PZT wet etch pattern, (h) After PZT wet etch, (i) After 25 min ash, (j) Oxide RIE pattern, (k) After oxide RIE, (l) After 25 min ash, (m) Ti/Au deposition pattern, (n) After Ti/Au deposition, (o) After acetone liftoff, and (p) XeF_2 etch releases cantilever.

3. Results and Discussion

X-ray diffraction was performed on a sample of the PT seed solution to determine the crystal orientation. For this test, a PT seed layer was deposited onto a 1 in. square Pt-coated silicon substrate with a thickness of approximately 250 nm. The plot in figure 6 shows a mixed texture of (001) and (110) oriented PT seed layer. The preferred seed layer should consist of solely (001) PT as the (001) orientation is required for templating a (001) oriented PZT thin film. Even with a mixed orientation, it is anticipated that the PT seed layer will lead to a greater degree of texturing within the PZT thin film.

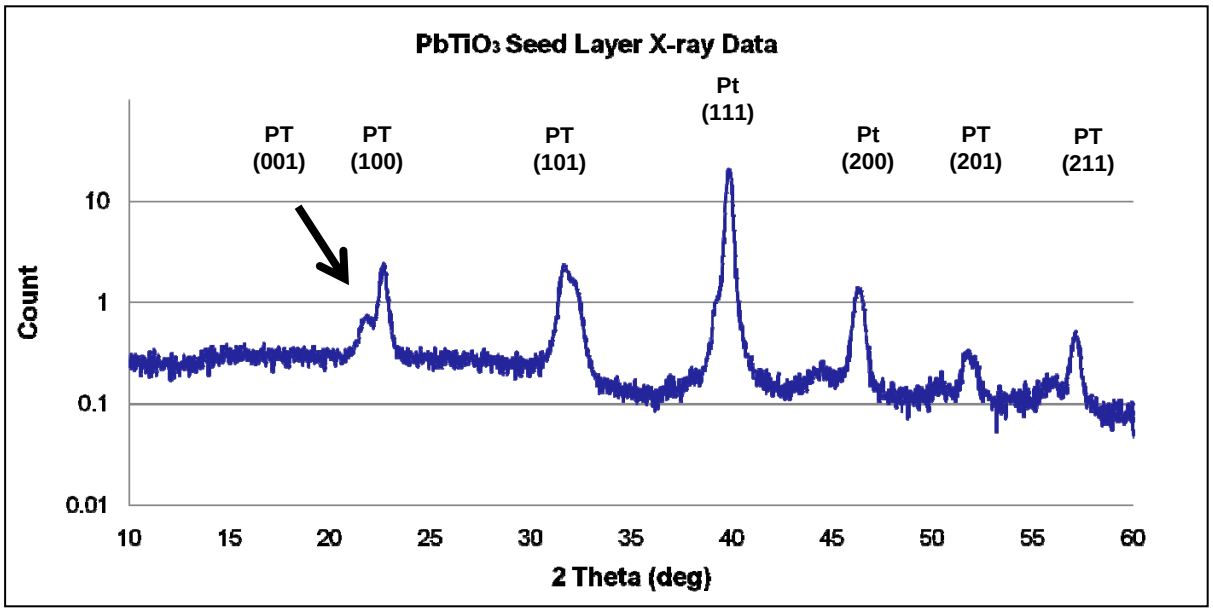

Figure 6. X-ray diffraction data for PT seed solution. (001) oriented crystals were confirmed.

A comparison was done on all PZT 45/55 samples with the PT seed solution and the control (figure 7). Samples 3 and 5 show decreased polarization values from the control while sample 7 exhibits similar values to the control. However, the dielectric constants of samples 3 and 4 are slightly higher from the control, see table 3.

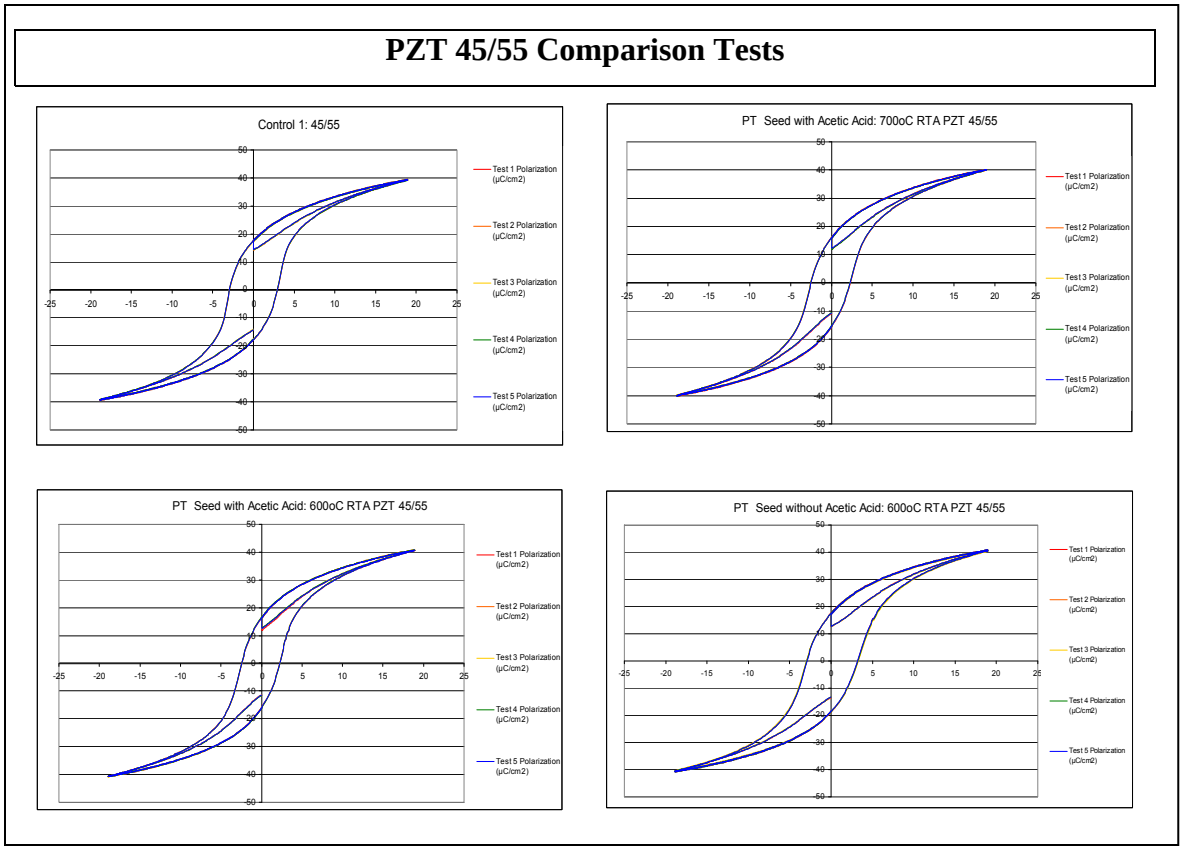

Figure 7. Comparison tests between all PZT 45/55 samples with PT seeds to the control PZT 45/55 sample.

Table 3. Summary of the ferroelectric and dielectric characterization on the eight 1-in. square test samples.

$PbTiO_3$ Seed Layer Test Measurements				
Sample		**Polarization + ($\mu C/cm^2$)**	**Polarization - ($\mu C/cm^2$)**	**Dielectric Constant**
1	Control 1: PZT (45/55)	17.68	17.56	1009
2	Control 2: PZT (52/48)	12.16	13.10	1179
3	PT Seed w/ CH_3COOH 700°C RTA PZT (45/55)	15.96	15.32	1137
4	PT Seed w/ CH_3COOH 700°C RTA PZT (52/48)	14.78	13.00	1299
5	PT Seed w/ CH_3COOH 600°C RTA PZT (45/55)	16.46	15.86	1187
6	PT Seed w/ CH_3COOH 600°C RTA PZT (52/48)	15.20	13.56	1354
7	PT Seed w/o CH_3COOH 700°C RTA PZT (45/55)	17.52	18.42	980
8	PT Seed w/o CH_3COOH 700°C RTA PZT (52/48)	15.86	17.02	988

The PZT 52/48 solution samples were also compared to the control sample without the PT seed solution (figure 8). Samples 4, 6, and 8 show increased polarization values. Sample 8 has a lower dielectric constant compared to the control sample; see table 3.

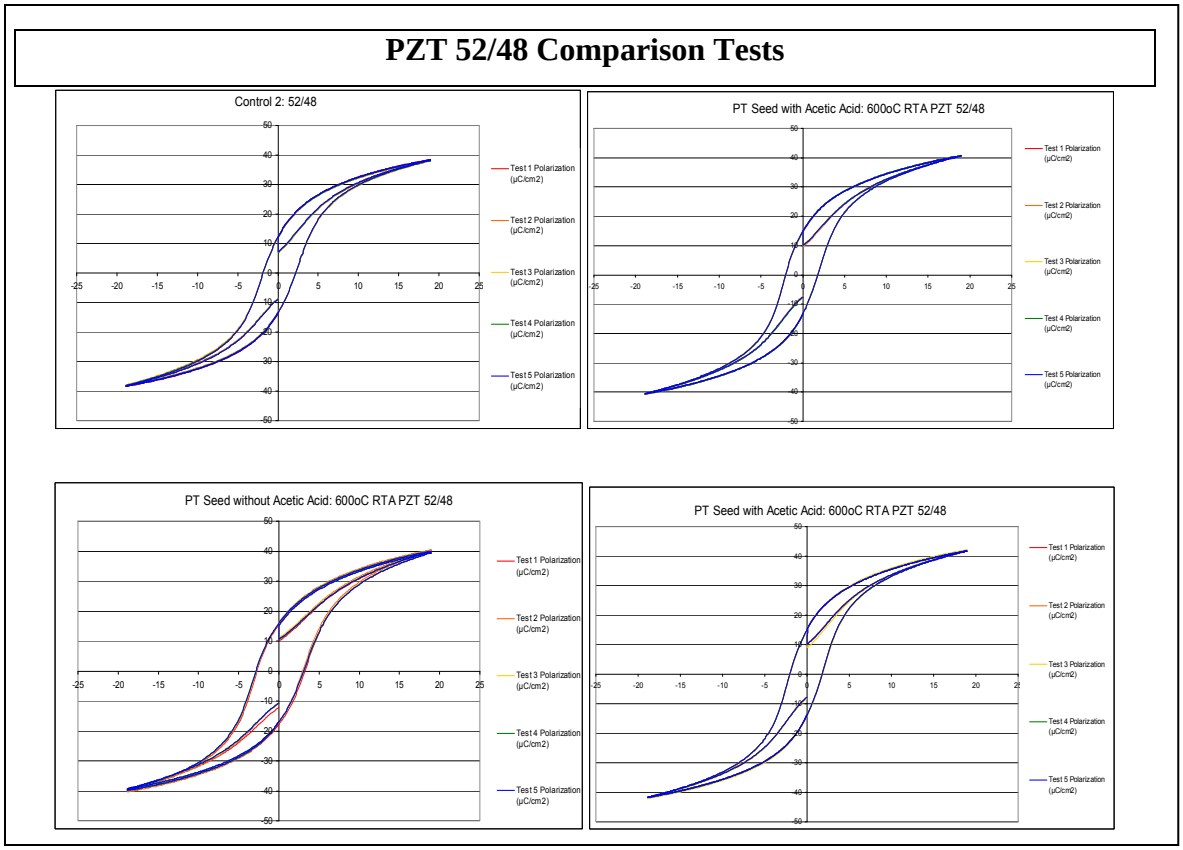

Figure 8. Comparison tests between all PZT 52/48 samples with PT seed layer to the control PZT 52/48 sample.

Samples 5, 6, 7, and 8 were compared since they all had similar PT seed layer RTA temperatures (figure 9). Samples 5 and 6 contained the seed layer with acetic acid while samples 7 and 8 were the samples without the acetic acid (see table 1). They all exhibit relatively similar polarization values; however, the dielectric constants of samples 5 and 6 are noticeable higher than those for the solutions without acetic acid.

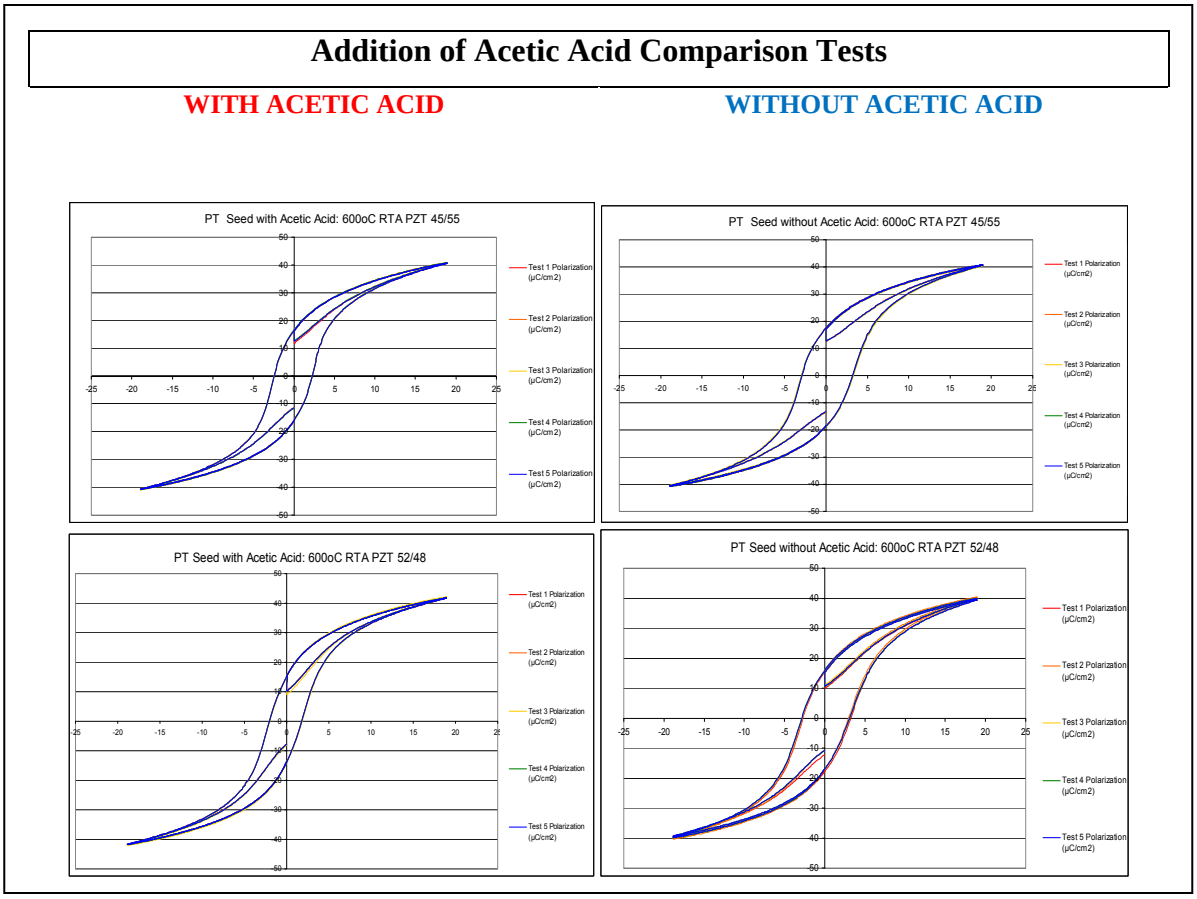

Figure 9. Comparison tests between samples with and without acetic acid.

After performing these tests, we were able to determine that the solutions used for samples 4 and 6 should be analyzed further. They both exhibited the highest dielectric constant with relatively narrow hysteresis loops along with a high remnant polarization.

After four wafers, containing PZT 52/48 standard solution, PZT 45/55 standard solution, PT seed layer with PZT 52/48 600 °C RTA, and PT seed layer with PZT 52/48 700 °C RTA, were fabricated, piezoelectric actuation comparison test data and hysteresis loops were collected using the optical profilometer in the backside laboratory. Data were collected from cantilevers 1, 2, and 3 (83 μm, 107 μm, and 132 μm lengths, respectively), see figure 10.

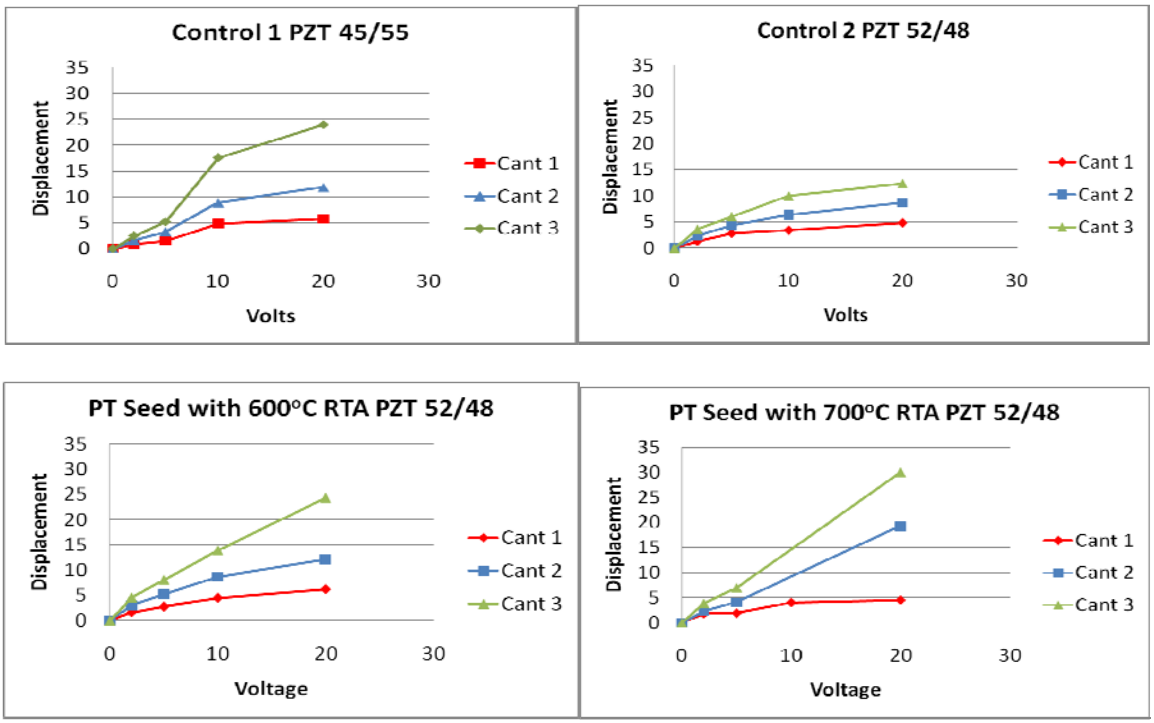

Figure 10. Cantilever displacement.

In previous studies PZT 45/55 has shown a higher piezoelectric coefficient compared to PZT 52/48 due to the random crystalline texture of the existing material. The two control samples demonstrate this once again (table 4). However, the two samples with the PT seed layer show noticeable improvements. There is a dramatic improvement, about double, in both PT seed layer samples over control sample 2 with PZT 52/48 and there is about a 20% improvement compared to control sample 1 with PZT45/55.

Table 4. Displacement values and the effective piezoelectric coefficient data (e_{31eff}).

Control Sample 1 - PZT 45/55						
V	Red		Blue		Green	
	Y	e_{31eff}	Y	e_{31eff}	Y	e_{31eff}
20	8.1	-6.7	15	-7.3	30.5	-9.7
10	7.2	-11.9	12	-11.6	23.0	-14.6
5	3.8	-12.5	6.4	-12.4	9.5	-12.1
2	3.2	-26.4	4.8	-23.2	6.8	-21.6
0	2.3	N/A	3.1	N/A	4.3	N/A

Control Sample 2 - PZT 52/48						
V	Red		Blue		Green	
	Y	e_{31eff}	Y	e_{31eff}	Y	e_{31eff}
20	6.6	-5.0	10.9	-4.9	15	-4.4
10	5.2	-7.9	8.5	-7.6	12.6	-7.4
5	4.6	-13.9	6.5	-11.6	8.7	-10.2
2	3.1	-23.5	4.5	-20.0	6.3	-18.4
0	1.8	N/A	2.1	N/A	2.7	N/A

PT Seed w/ Acetic Acid 600°C RTA - PZT 52/48						
V	Red		Blue		Green	
	Y	e_{31eff}	Y	e_{31eff}	Y	e_{31eff}
20	9.2	-6.6	17.5	-7.3	33.8	-9.3
10	7.5	-10.7	14	-11.7	21.4	-11.8
5	5.8	-16.5	10.5	-17.6	15.6	-17.2
2	4.6	-32.8	8.4	-35.2	12.1	-33.3
0	3	N/A	5.3	N/A	7.5	N/A

PT Seed with Acetic Acid 600°C RTA - PZT 52/48						
V	Red		Blue		Green	
	Y	e_{31eff}	Y	e_{31eff}	Y	e_{31eff}
20	8	-5.7	21.3	-9.0	32.3	-8.9
10	7.5	-10.8	16.6	-14.0	24.8	-13.7
5	5.4	-15.5	9.6	-16.2	14.9	-16.5
2	5.3	-38.0	7.8	-32.9	11.8	-32.7
0	3.5	N/A	5.5	N/A	7.9	N/A

Control sample 1 with PZT 45/55 and control sample 2 with PZT 52/48 demonstrate standard e_{31} values compared to previous literature. The new samples with the PT seed solutions show elevated e_{31} values compared to control sample 2. The PT seed samples show only a slight improvement compared to control sample 1. This confirms the previous findings that there is a notable improvement in the PZT solutions through the use of the PT seed.

Comparing the hysteresis graphs of all samples after piezoelectric actuation tests (figure 11), the two samples with the PT seed layer show slightly more narrow curves than both control sample 1 and 2. They also show higher polarization values than control samples 2 with PZT 52/48 and similar values to control sample 1 with PZT 45/55. This also confirms the previous findings by PSU.

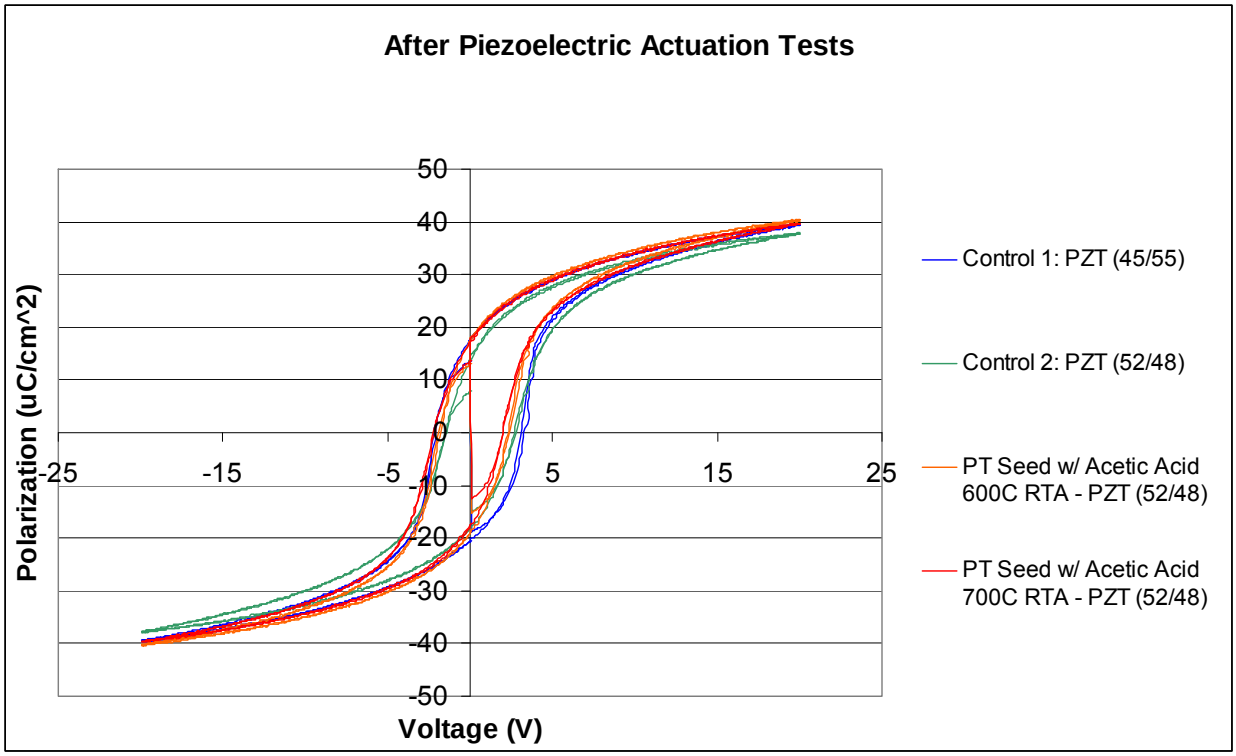

Figure 11. Comparison of all samples after piezoelectric actuation tests.

4. Summary and Conclusions

X-ray diffraction data shows a mixed texture of (001) and (110) oriented PT seed layers instead a strongly textured (001) orientation. One possible explanation is that small amounts of TiO_2 have infiltrated the Pt electrode resulting in the nucleation of non-(001) oriented grains of lead titanate.

After analyzing the first hysteresis data for the $PbTiO_3$ seed layer tests using eight 1-in. samples, we decided to continue the tests on two 100 mm wafers. The solutions that were used were a PT seed with acetic acid 600 °C RTA PZT (52/48) and a PT seed with acetic acid 700 °C RTA PZT (52/48) (solutions 4 and 6, respectively).

Once the wafers were completed they were removed from the cleanroom and taken to the backside labs to undergo more electrical measurements. Using the optical profilometer the samples underwent ferroelectric and piezoelectric actuation tests. The results demonstrated increased piezoelectric displacement values for both PT seed samples compared to the control sample with PZT 52/48 and PZT 45/55. They also show narrow hysteresis loops with higher polarization values than PZT 52/48.

Greater improvements can be expected for a PT seed with a strong (001) orientation. Work will continue on the PT seed layer and the Ti/Pt base metallization to achieve a stronger (001) orientation and ultimately a doubling in the piezoelectric coefficient of PZT.

5. References

1. Prume, K.; Muralt, P.; Calame, F.; Schmitz-Kempen, T.; Tiedke, S. *IEEE Transactions on Ultrasonics, Ferroelectrics, and Frequency Control* **2007**, *54*, 8–14.
2. Polcawich, R.; Judy, D.; Pulskamp, J.; Trolier-McKinstry, S.; Dubey, M. *IEEE* **2007**, 2083–2086.
3. Physik Instrumente, http://www.physikinstrumente.com/en/index.php (access August 2008).
4. Muralt, P.; Maeder, T.; Sagalowicz, L.; et al. *Journal of Applied Physics* **1998**, *83*, 3835–3841.
5. Hiboux, S.; Muralt, P. *Journal of the European Ceramic Society* **2004**, *24*, 1593–1596.
6. Trolier-McKinstry, S. *Improved Thin Film Piezoelectrics for Actuator Applications*. ARO-STIR, FY07.
7. Prume, K.; Muralt, P.; Calame, F.; Schmitz-Kempen, T.; Tiedke, *J. Electroceramics* **2007**, *17*, 407–411.
8. Trolier –McKinstry, S. (Pennsylvania State University), private communication, 2008.
9. Piekarz, R. *Lead Zirconate Titanate (PZT) Sol-Gel Thin Film Preparation, Deposition and Testing*; ARL-02-02; U.S. Army Research Laboratory: Adelphi, MD, 2002.
10. Madou, M. J. *Fundamentals of Microfabrication*, CRC Press, Baca Raton, FL, 1988.

Acronyms and Abbreviations

2-MOE	2-Methoxyethanol
ARL	U.S. Army Research Laboratory
ATO	Army Research Office
MEMS	microelectromechanical systems
N_2	nitrogen
PECVD	plasma enhanced chemical vapor deposition
PSU	Pennsylvania State University
PT seed layer	$PbTiO_3$ seed layer
Pt	platinum
PZT	lead zirconate titanate
RTA	Rapid Thermal Anneal
STIR	Short Term Innovative Research
Ti	titanium
Zr	zirconium

No. of Copies	Organization
1 ELECT	ADMNSTR DEFNS TECHL INFO CTR ATTN DTIC OCP 8725 JOHN J KINGMAN RD STE 0944 FT BELVOIR VA 22060-6218
1	DARPA ATTN IXO S WELBY 3701 N FAIRFAX DR ARLINGTON VA 22203-1714
1 CD	OFC OF THE SECY OF DEFNS ATTN ODDRE (R&AT) THE PENTAGON WASHINGTON DC 20301-3080
1	US ARMY RSRCH DEV AND ENGRG CMND ARMAMENT RSRCH DEV AND ENGRG CTR ARMAMENT ENGRG AND TECHNLG Y CTR ATTN AMSRD AAR AEF T J MATTS BLDG 305 ABERDEEN PROVING GROUND MD 21005-5001
1	PM TIMS, PROFILER (MMS-P) AN/TMQ-52 ATTN B GRIFFIES BUILDING 563 FT MONMOUTH NJ 07703
1	US ARMY INFO SYS ENGRG CMND ATTN AMSEL IE TD F JENIA FT HUACHUCA AZ 85613-5300
1	COMMANDER US ARMY RDECOM ATTN AMSRD AMR W C MCCORKLE 5400 FOWLER RD REDSTONE ARSENAL AL 35898-5000
1	US GOVERNMENT PRINT OFF DEPOSITORY RECEIVING SECTION ATTN MAIL STOP IDAD J TATE 732 NORTH CAPITOL ST NW WASHINGTON DC 20402

No. of Copies	Organization
1	US ARMY RSRCH LAB ATTN AMSRD ARL CI OK TP TECHL LIB T LANDFRIED BLDG 4600 ABERDEEN PROVING GROUND MD 21005-5066
1	DIRECTOR US ARMY RSRCH LAB ATTN AMSRD ARL RO EV W D BACH PO BOX 12211 RESEARCH TRIANGLE PARK NC 27709
16	US ARMY RSRCH LAB ATTN AMSRD ARL CI OK PE TECHL PUB ATTN AMSRD ARL CI OK TL TECHL LIB ATTN AMSRD ARL SE R P AMIRTHARAJ ATTN AMSRD ARL SE RL B PIEKARSKI ATTN AMSRD ARL SE RL L SANCHEZ (3 COPIES) ATTN AMSRD ARL SE RL M DUBEY ATTN AMSRD ARL SE RL R POLCAWICH (7 COPIES) ATTN IMNE ALC IMS MAIL & RECORDS MGMT ADELPHI MD 20783-1197
TOTAL:	26 (24 HC, 1 CD, 1 Elec)